The role of *floral organs in carpels*, an Arabidopsis loss-of-function mutation in *MicroRNA160a*, in organogenesis and the mechanism regulating its expression

Xiaodong Liu[1],[†],[‡], Jian Huang[1],[†], Yao Wang[1], Kanhav Khanna[2], Zhixin Xie[2], Heather A. Owen[1] and Dazhong Zhao[1],[*]

[1]*Department of Biological Sciences, University of Wisconsin-Milwaukee, Milwaukee, WI 53211, USA, and*
[2]*Department of Biological Sciences, Texas Tech University, Lubbock, TX 79409, USA*

SUMMARY

MicroRNAs (miRNAs) have emerged as key regulators of gene expression at the post-transcriptional level in both plants and animals. However, the specific functions of *MIRNA*s (*MIR*s) and the mechanisms regulating their expression are not fully understood. Previous studies showed that miR160 negatively regulates three genes that encode AUXIN RESPONSE FACTORs (ARF10, -16, and -17). Here, we characterized *floral organs in carpels* (*foc*), an Arabidopsis mutant with a *Ds* transposon insertion in the 3′ regulatory region of *MIR160a*. *foc* plants exhibit a variety of intriguing phenotypes, including serrated rosette leaves, irregular flowers, floral organs inside siliques, reduced fertility, aberrant seeds, and viviparous seedlings. Detailed phenotypic analysis showed that abnormal cell divisions in the basal embryo domain and suspensor led to diverse defects during embryogenesis in *foc* plants. Further analysis showed that the 3′ region was required for the expression of *MIR160a*. The accumulation of mature miR160 was greatly reduced in *foc* inflorescences. In addition, the expression pattern of *ARF16* and *-17* was altered during embryo development in *foc* plants. *foc* plants were also deficient in auxin responses. Moreover, auxin was involved in regulating the expression of *MIR160a* through its 3′ regulatory region. Our study not only provides insight into the molecular mechanism of embryo development via *MIR160a*-regulated *ARF*s, but also reveals the mechanism regulating *MIR160a* expression.

Keywords: microRNA, *MicroRNA160a*, organogenesis, embryogenesis, *AUXIN RESPONSE FACTOR*, auxin.

INTRODUCTION

MicroRNAs (miRNAs) are small (∼21 nucleotides) non-coding RNAs that are key post-transcriptional controllers of gene expression in both plants and animals. MicroRNAs regulate gene expression by guiding the cleavage of target mRNAs or attenuating the translation of their target genes (Bartel and Bartel, 2003; Carrington and Ambros, 2003; Jones-Rhoades *et al.*, 2006; Chen, 2008; Bartel, 2009; Voinnet, 2009). In plants, primary miRNAs (pri-miRNAs) are transcribed from *MIRNA* (*MIR*) genes. Stem–loop segments derived from pri-miRNAs are cleaved by RNase III-type endonucleases (Dicer) to produce paired miRNAs with approximately 21 nucleotides, including two-nucleotide 3′ overhangs. After liberation of the miRNA duplexes, mature miRNAs are loaded into an RNA-induced silencing complex (RISC), where they interact with target mRNAs by comple-

mentary matching for cleavage or translational attenuation. The general functions of miRNAs have mainly been revealed by analyzing mutants that are impaired in miRNA biogenesis, such as *dcl1* (Park *et al.*, 2002; Kurihara and Watanabe, 2004), *ago* (Kidner and Martienssen, 2004; Baumberger and Baulcombe, 2005), *hen1* (Boutet *et al.*, 2003), *hyl1* (Song *et al.*, 2007), *se* (Grigg *et al.*, 2005; Yang *et al.*, 2006), and *ddl* (Yu *et al.*, 2008) mutants. The specific functions of miRNAs are primarily established through gain-of-function appro-aches, including ectopic expression of miRNAs and expression of miRNA-resistant versions of their targets. So far, only a handful of loss-of-function mutants with detect-able phenotypes have been identified in *MIR*s in plants and other organisms (Miska *et al.*, 2007; Voinnet, 2009). In addi-tion, the temporal and spatial actions of miRNAs have not

been extensively studied. Therefore, it is of great importance to investigate the function of individual miRNAs and the mechanisms controlling *MIR* gene expression.

Auxin is essential for plant vegetative growth and reproductive development. AUXIN RESPONSE FACTORs (ARFs), which are released by the auxin receptor E3 ubiquitin ligase complex SCF^{TIR1}, regulate the expression of a large set of auxin-responsive genes by binding to auxin response elements (AuxREs) in their promoters (Guilfoyle and Hagen, 2007; Mockaitis and Estelle, 2008). Among 23 *ARF*s in Arabidopsis, recent studies showed that miRNAs and *trans*-acting-small interfering RNAs (ta-siRNAs) play important roles in controlling transcript abundance of *ARF2, -3, -4, -6, -8, -10, -16,* and *-17* (Okushima *et al.*, 2005; Guilfoyle and Hagen, 2007). The trans-acting small interfering RNA ARFs (tasiR-ARFs) target *ARF2, -3,* and *-4* (Allen *et al.*, 2005; Williams *et al.*, 2005; Fahlgren *et al.*, 2006). The gradient of tasiR-ARFs established by small RNA movement is critical for patterning ARF3 in leaf development (Chitwood *et al.*, 2009). The expression of *ARF6* and *-8* is regulated by miR167, which is essential for anther and ovule development (Wu *et al.*, 2006). Furthermore, gain-of-function analyses showed that miR160 is important for plant development by negatively regulating the expression of *ARF10, -16,* and *-17* (Mallory *et al.*, 2005; Wang *et al.*, 2005; Liu *et al.*, 2007). Based on transient expression experiments and protein structures, ARFs 5–8, and 19 may function as transcriptional activators, while ARFs 1–4, 9–18, and 20–22 possibly act as repressors (Ulmasov *et al.*, 1999; Tiwari *et al.*, 2003; Okushima *et al.*, 2005). So far, only *ARF5* (*MONOPTEROS*) and *ARF7* (*NON-PHOTOTROPIC HYPOCOTYL4*) have been shown to play direct roles in embryogenesis (Hardtke and Berleth, 1998; Harper *et al.*, 2000; Hamann *et al.*, 2002; Hardtke *et al.*, 2004). Plants expressing a miR160-resistant version of *ARF17* produced aberrant seedlings, suggesting that miR160 may control early embryo development (Mallory *et al.*, 2005). miR160 is derived from three genes: *MIR160a, -b,* and *-c*. However, it is not clear how a specific *MIR160* regulates plant development, particularly embryo development, by post-transcriptional regulation of *ARF10, -16,* and *17*.

Arabidopsis has about 190 *MIR* genes (http://www.mirbase.org). To date, the function of only a few miRNAs has been studied by loss-of-function analysis (Vaucheret *et al.*, 2004; Baker *et al.*, 2005; Gasciolli *et al.*, 2005; Guo *et al.*, 2005; Allen *et al.*, 2007; Cartolano *et al.*, 2007; Sieber *et al.*, 2007; Nag *et al.*, 2009; Wu *et al.*, 2009). For example, *mir159a* or *mir159b* single mutants have no phenotypes, while the *mir159ab* double mutant exhibited diverse abnormalities, including reduced apical dominance, curled leaves, reduced fertility, and small seeds (Allen *et al.*, 2007). *eep1*, which is impaired in *MIR164c* function, produced extra petals in early flowers (Baker *et al.*, 2005). Both *mir164a* and *mir164b* single mutants formed more lateral roots (Guo *et al.*, 2005). Anal-

ysis of the *mir164abc* triple mutant uncovered functional redundancy and specialization among three *MIR164* genes (Sieber *et al.*, 2007). Here, we characterize a miRNA loss-of-function mutant, *floral organs in carpels* (*foc*), in which the *MIR160a* gene is disrupted by a *Ds* transposon insertion in its 3′ regulatory region. *foc* plants exhibited a wide range of intriguing phenotypes in leaf, flower, embryo, and seed development. We demonstrate that the 3′ region of *MIR160a* is required for its expression pattern. During embryogenesis in *foc* plants, abnormal cell divisions in the basal embryo domain and suspensor cause various embryonic defects mainly due to the altered expression pattern of *ARF16* and *-17*. *foc* plants are also deficient in auxin responses. Moreover, auxin regulates the expression of *MIR160a*, possibly through potential auxin response elements in its 3′ regulatory region. Our results suggest that *MIR160a* is required for the development of multiple organs, particularly the embryo, through a mechanism involving auxin signaling.

RESULTS

foc has defective flower development

To identify those genes important for reproductive development using the loss-of-function approach, we screened Arabidopsis *Ds* transposon insertion lines (Sundaresan *et al.*, 1995; Zhao *et al.*, 2002; Jia *et al.*, 2008). One mutant showed interesting phenotypes in both vegetative and reproductive development. Besides producing serrated rosette leaves (Figure S1 in Supporting Information), the mutant plants exhibited diverse abnormalities in reproductive development, including flower development. The mutant plants produced abnormal flowers with long pedicles (Figures 1a,b and S2a,b). Wild-type buds are enclosed by sepals and open flowers have four sepals, four petals, six stamens, and two fused carpels (Figure 1a,c,g). However, the mutant plants frequently formed buds with unfurled sepals (Figure 1b,h). Seventy per cent of the mutant flowers had narrow sepals and petals (Figure 1d), and flowers produced in late stages had variable numbers of floral organs (Figures 1e and S2e–h). In short-day conditions, 30% of the first 10 mutant siliques became swollen (Figure 1f). More strikingly, floral organs formed inside these swollen carpels (Figures 1i and S2i–k). We therefore named this mutant *floral organs in carpels* (*foc*). Eventually, inflorescences emerged from siliques (Figures 1j and S2i). Our results suggest that *FOC* plays important roles in controlling floral organ identity and formation.

foc has abnormal seed and embryo development

foc plants are defective in seed development and exhibit reduced fertility (Figure S3a–e). Compared with wild-type seeds, *foc* seeds are variable in size (Figure S3f,g). Moreover, *foc* plants show a viviparous phenotype (Figure S3c–i). Semi-thin sectioning revealed various abnormalities in late
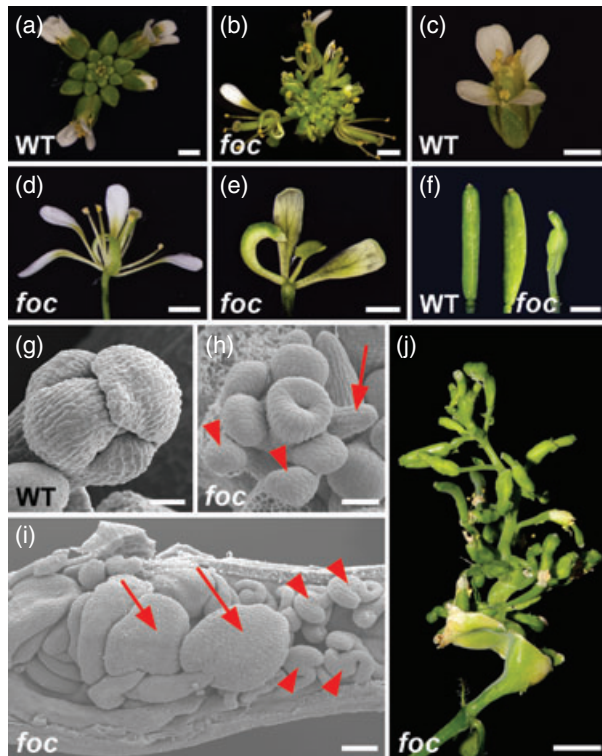
Figure 1. *foc* has defective flower development.
(a) A wild-type inflorescence. (b) A *foc* inflorescence showing flowers with unfurled sepals. (c) A wild-type flower. (d) A *foc* flower exhibiting narrow sepals and petals. (e) A *foc* flower showing one sepal-like, two petal-like, and one stamen-like structures. (f) Developing wild-type silique (left) and two *foc* swollen siliques (middle and right). (g) Scanning electron microscope (SEM) image showing a wild-type stage 7 bud enclosed by sepals. (h) A SEM image showing an unfurled *foc* stage 7 bud, indicated by stalks on stamen primordia and the slotted tube of the gynoecium (arrowheads, sepal primordia; arrow, a filamentous structure). (i) A SEM image showing floral organs generated inside a *foc* silique (arrows, stamen-like structures; arrowheads, ovules). (j) An emerged inflorescence from a *foc* silique.
Scale bars: 1 mm in (a–f), (j); 25 μm in (g, h); 50 μm in (i).

seed development (Figure S3j–m), which cause diverse defects in young seedlings (Figure S4).

The seed and seedling phenotypes suggest that *foc* plants are defective in early embryo development. Therefore, we analyzed embryo development by preparing whole-mount squashes of embryos. Wild-type embryo development is initiated from a zygote. Lineages with different developmental fates are initially established by producing a small, spherical apical (or terminal) cell and a large elongated basal cell (West and Harada, 1993; Laux *et al.*, 2004). The first round of cell division in the apical and basal cells results in the formation of a two-celled embryo consisting of an embryo proper and a suspensor (Figure 2a). Subsequent cell divisions give rise to embryos at the octant (eight cells, Figure 2b), dermatogen (16-cells, Figure 2c), globular (Figure 2d), triangular (or transition, Figure 2e), heart (Figure 2f), torpedo (Figure S3j), and bent cotyledon stages

(Figure S3l). However, abnormal embryo development in *foc* occurred at the very beginning of embryogenesis. In wild-type embryos, the suspensor contains a single file of cells that are derived from a series of transverse divisions of the basal cell (Figure 2a–e). In *foc* embryos, at the two- to four-cell stage, suspensor cells appeared to divide both transversely and longitudinally, resulting in the formation of a double-filed suspensor (Figure 2g). Furthermore, the mutant embryo proper failed to differentiate normally, leading to a non-spherical and asymmetric embryo at the octant stage (Figure 2h). *foc* embryos did not form normal hypophyses due to abnormal cell divisions in both the suspensor and embryo proper (Figure 2i,j). These early defects caused aberrant embryos in later stages (Figure 2k,l).

By analyzing embryos at specific times after fertilization, we found that the distribution of *foc* embryos at different stages was significantly different from that of wild type (Table 1). By 2 days after pollination (DAP), most wild-type embryos (93% or 119/128) had reached the dermatogen and globular stages, while only 7% (9/128) of embryos were at the quadrant and octant stages (Table 1). In contrast, by 2 DAP, 51% (45/88) of *foc* embryos were still at the quadrant or octant stage (Table 1). After 2 DAP, besides morphological defects, the development of *foc* embryos was more severely retarded and developmental stages were widely distributed (Table 1). In summary, abnormal cell divisions in the basal embryo domain and uppermost part of the suspensor caused various defects during embryogenesis in *foc* plants. Furthermore, embryo development in *foc* plants was severely retarded and asynchronous.

FOC is *MIR160a*

To identify *FOC*, we first performed genetic analyses. Wild-type plants were crossed to *foc* plants. All F$_1$ plants exhibited the wild-type phenotype, suggesting that *foc* is recessive. In the F$_2$ generation, approximately one quarter (55 mutant: 171 wild type) of the plants displayed mutant phenotypes, indicating that these diverse phenotypes may be caused by a single gene mutation. However, thermal asymmetric interlaced (TAIL)-PCR (Liu *et al.*, 1995; Zhao *et al.*, 2002) revealed two *Ds* insertion sites within 6198 bp of each other (Figure S5a). One *Ds* (designated *Ds1*) was located 835 bp upstream of the ATG start codon of *At2g39170* (Figure S5a), which encodes an unknown protein. The other *Ds* (*Ds2*) was located downstream of *MIR160a* (*At2g39175*) (Figure S5a). We cloned the 967-bp full-length transcript of *MIR160a* by 5′ and 3′ rapid amplification of cDNA ends (RACE)-PCR (Figure S6) and determined that the *Ds2* insertion was 1635 bp from the 3′ region of *MIR160a*.

Our RT-PCR results demonstrated that *MIR160a* was expressed in seedlings, stems, roots, inflorescences, and mature leaves in wild-type plants (Figure S5b). However, in *foc*, the *MIR160a* transcript was not detected in stems,
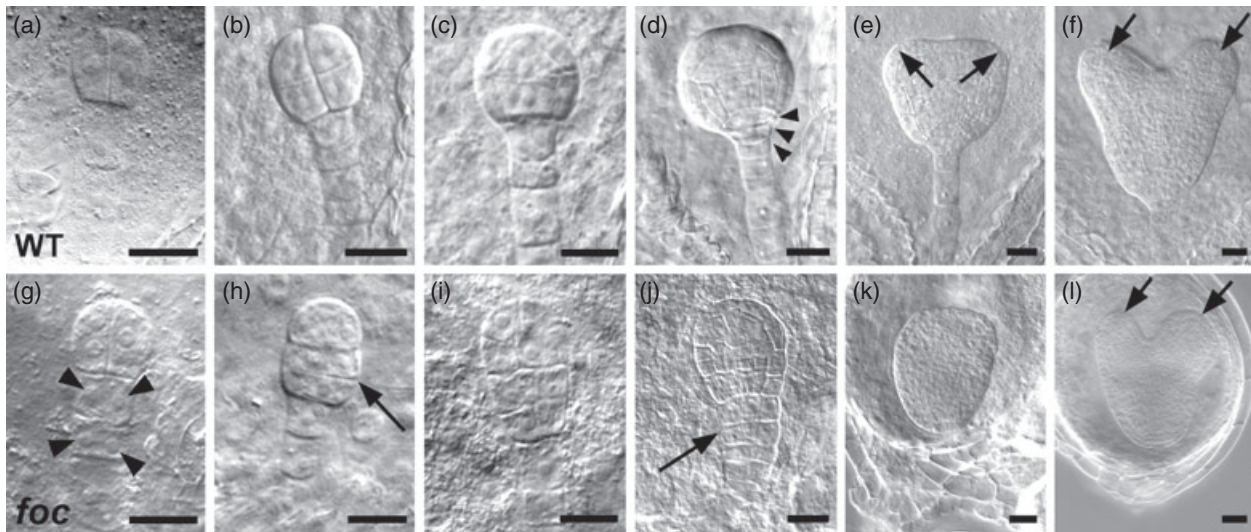
Figure 2. *foc* has defective early embryo development.

(a, g) A wild-type embryo at the two to four cell stage, showing a longitudinal cell division in the apical cell and transverse cell division in suspensor cells (a) while a *foc* embryo shows aberrant longitudinal cell divisions in suspensor cells, resulting in a double-filed suspensor (g, arrowheads).

(b, h) A wild-type embryo at the octant (eight cell) stage exhibiting an embryo proper resulting from both transverse and longitudinal cell divisions, and a single-filed suspensor resulting exclusively from transverse cell divisions (b), while a *foc* embryo shows abnormal cell divisions in central and basal embryo domains (h, arrow).

(c, i) A wild-type embryo at the dermatogen stage (16 cell, c); while a *foc* embryo at the dermatogen-like stage shows abnormal cell divisions in the embryo proper (i).

(d, j) A wild-type embryo at the globular stage showing hypophysis (d, arrowheads), while a *foc* embryo at the globular-like stage shows a triple-filed suspensor (j, arrow), but no typical hypophysis.

(e, k) A wild-type embryo at the triangular (transition) stage, showing cotyledon buttresses (e, arrows), while a *foc* embryo at the triangular-like stage has no suspensor (k).

(f, l) A wild-type embryo at the heart stage, showing enlarged cotyledon lobes (f, arrows), while a *foc* embryo at the heart-like stage shows two asymmetric cotyledon lobes (l, arrows).

Scale bars: 25 μm in (a–l).

Table 1 Comparison of embryogenesis between wild-type and *foc* plants. Siliques from wild-type and *foc* plants were dissected. Whole-mount preparations of embryos were cleared and examined and the numbers of embryos at each developmental stage were recorded

DAP	Genotype	Quadrant or octant	Dermatogen	Globular	Triangular	Heart	Torpedo	Bent cotyledon	Mature or desiccation
2	wt	9	62	57					
	foc	45	37	6					
3	wt			5	56	70			
	foc	8	22	54	17	7			
4	wt					19	95	8	
	foc		11	33	19	16	3		6
5	wt						34	99	
	foc			4	12	10	4	22	44
7	wt								145
	foc					2		3	102

DAP, days after pollination.

inflorescence, or mature leaves. In young seedlings, *MIR160a* expression was decreased, while its expression in roots appeared normal. Our results indicate that *Ds2* severely disrupts the expression of *MIR160a*.

Due to the linkage of two *Ds* insertions, we performed complementation experiments. Two constructs, *ETA* and *ETB*, harboring a 3820 bp genomic DNA fragment for *At2g39170* and a 4921 bp fragment for *MIR160a* (*At2g39175*) respectively, were generated to create transgenic plants. Thirty PCR-verified transgenic plants for each construct were chosen to cross with +/*foc* plants. In 23 F₂ populations, plants with the *ETB* transgene exhibited a wild-type phenotype in the *foc* background, after PCR verifications. Conversely, every plant carrying the *ETA* transgene
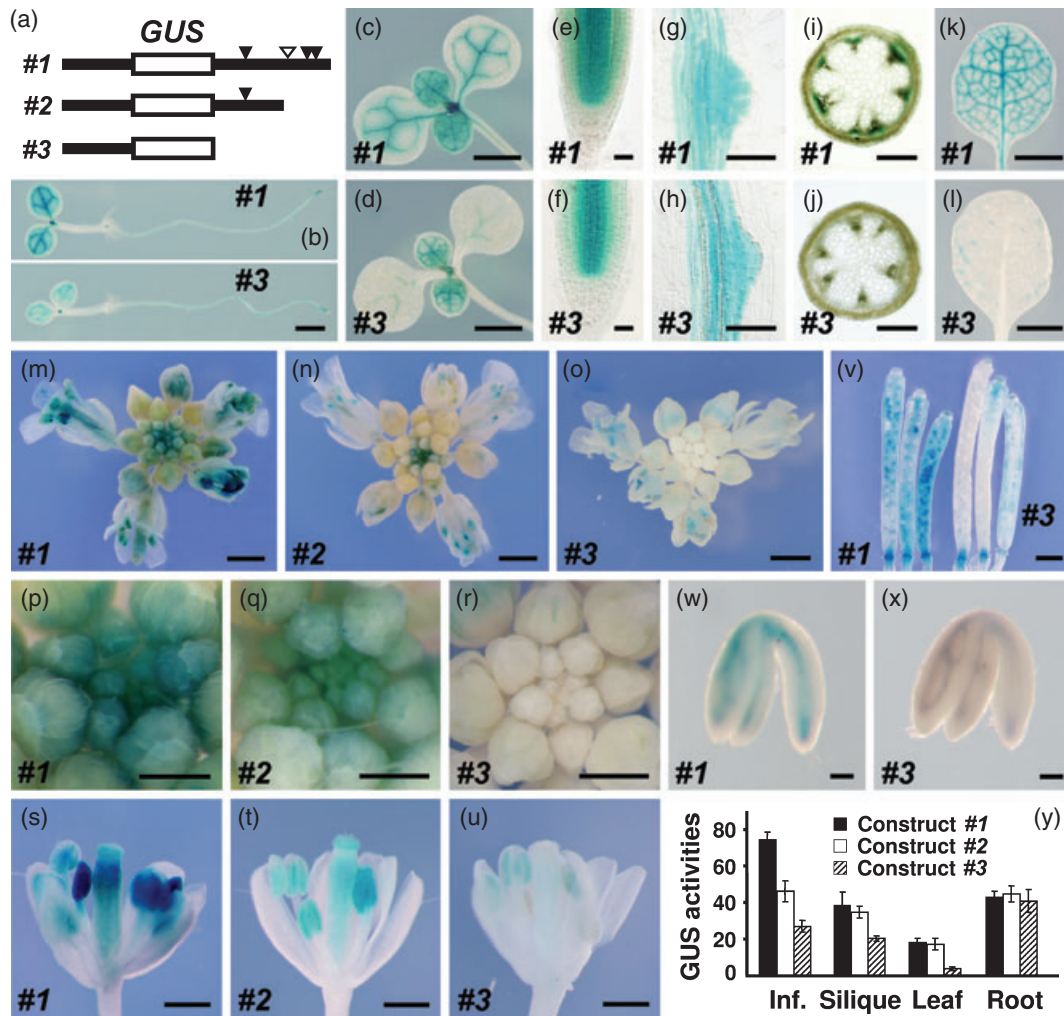
Figure 3. The 3′ region of *FOC* is required for its expression pattern.

(a) A diagram showing three constructs: #1, *Pro*_{FOC}:GUS:*3′*_{FOC}; #2, *Pro*_{FOC}:GUS:*Δ3′*_{FOC}; and #3, *Pro*_{FOC}:GUS (open arrowhead indicates the site of the *Ds* insertion in the 3′ region of *foc*, while solid arrowheads indicate the positions of three potential auxin response elements in the 3′ region of *FOC*). (b) A *Pro*_{FOC}:GUS:*3′*_{FOC} young seedling (top) expressing GUS at similar level in root, but at a higher level in cotyledons, relative to expression levels in a *Pro*_{FOC}:GUS plant (bottom). (c, d) GUS activity was higher in cotyledons and young true leaves of *Pro*_{FOC}:GUS:*3′*_{FOC} seedlings (c) than that of *Pro*_{FOC}:GUS (d). (e–h) *Pro*_{FOC}:GUS:*3′*_{FOC} plants with similar GUS expression patterns in root tip (e) and lateral root (g) as in *Pro*_{FOC}:GUS plants (f, h). (i, j) GUS staining in stem vascular bundles of *Pro*_{FOC}:GUS:*3′*_{FOC} plants (i), but not of *Pro*_{FOC}:GUS plants (j). (k, l) GUS staining in mature true leaves of *Pro*_{FOC}:GUS:*3′*_{FOC} (k), but almost undetectable in *Pro*_{FOC}:GUS leaves (l). (m–r) GUS staining of inflorescences showing strong expression in *Pro*_{FOC}:GUS:*3′*_{FOC} young buds and open flowers (m, p), with GUS signal but greatly reduced expression in *Pro*_{FOC}:GUS:*Δ3′*_{FOC} (n, q). In *Pro*_{FOC}:GUS plants, GUS activity was almost undetectable in young buds and markedly reduced in open flowers (o, r). (s–u) Relative to expression in *Pro*_{FOC}:GUS:*3′*_{FOC} flower (s), GUS activity in carpels was reduced in *Pro*_{FOC}:GUS:*Δ3′*_{FOC} (t) and *Pro*_{FOC}:GUS flowers (u). (v–x) GUS signal in *Pro*_{FOC}:GUS:*3′*_{FOC} embryos (v, left three and w), but not in *Pro*_{FOC}:GUS embryos (v, right three and x). (y) Quantification of GUS activity (nM 4-methylumbelliferone (4-MU)/min/mg).

Abbreviation: Inf., inflorescence. Scale bars: 1 mm in (b–d, m–o), (v); 50 μm in (e–h), (w, x); 0.5 mm in (i, j), (p–u); 0.5 cm in (k, l).

still had *foc* phenotypes in the *foc* background. Taken together, our results strongly suggest that *Ds2* inserted in the 3′ region of *MIR160a* is responsible for the *foc* phenotypes.

The 3′ region of *FOC* is required for its expression pattern

To further determine whether the 3′ region is required for the *FOC* expression, we generated three constructs using the GUS reporter gene (Figure 3a). By analyzing plants expressing a *Pro*_{FOC}:GUS:*3′*_{FOC} (Figure 3a, #1, wild-type version) transgene, we found that *FOC* was expressed in cotyledons, roots, and rosette leaves of young seedlings (Figure 3b top, c). *FOC* was also strongly expressed in root tips (Figure 3e), lateral roots (Figure 3g), stems (Figure 3i), vascular tissues of mature leaves (Figure 3k), and in young buds and open flowers (Figure 3m,p). *FOC* was primarily expressed in anthers and carpels (Figure 3s) as well as in developing embryos (Figure 3v, leftmost three, w). Our results indicate that *FOC* is expressed in all organs, especially in reproductive organs.

Transgenic plants harboring *Pro$_{FOC}$*:GUS (Figure 3a, #3, lacking the 3′ region) and *Pro$_{FOC}$*:GUS:*Δ3′$_{FOC}$* (Figure 3a, #2, with a partial 3′ region) showed GUS staining patterns different from plants expressing *Pro$_{FOC}$*:GUS:*3′$_{FOC}$*. In *Pro$_{FOC}$*:GUS plants, GUS staining in the young seedling roots (Figure 3b bottom), root tips (Figure 3f), and lateral roots (Figure 3h) was similar to that of *Pro$_{FOC}$*:GUS:*3′$_{FOC}$* (Figure 3b top, e,g). However, GUS activity was reduced in cotyledons and young rosette leaves (Figure 3b bottom, d). Almost no GUS activity was detected in stems (Figure 3j), mature leaves (Figure 3l), young buds (Figure 3o,r), carpels (Figure 3u), and developing embryos (Figure 3v right three, x). *Pro$_{FOC}$*:GUS:*Δ3′$_{FOC}$* plants showed reduced GUS staining intensities when compared with *Pro$_{FOC}$*:GUS:*3′$_{FOC}$* (Figure 3n,q,t) plants. The quantification of GUS activity confirmed the results from GUS staining (Figure 3y). Our results indicate that the 3′ regulatory region of *FOC* is required for its expression in aerial organs, particularly in reproductive organs, including flowers and embryos.

The accumulation of mature miR160 and expression of *ARF10, -16, and -17* are altered in *foc* plants

To examine the effect of the *foc* mutation on overall accumulation of mature miR160, we performed small RNA Northern blot assays. In the wild type, miR160 was readily detected in both leaves and inflorescences, with higher levels in the inflorescences (Figure 4a). However, miR160 was substantially reduced in *foc* leaves and inflorescences (Figure 4a). Accumulation of miR160 showed a 72% reduction in *foc* inflorescences, relative to levels in wild type, while a 21% reduction was found in leaves (Figure 4b), suggesting that the *foc* mutation has a more profound effect on miR160 homeostasis in the inflorescence. The effect of the *foc* mutation on accumulation of miRNA appeared to be specific to miR160, since the accumulation of miR168 was not affected in either leaves or inflorescences (Figure 4c,d). The accumulation of miR171 was also found to be unaffected by the *foc* mutation (data not shown).

To test whether the altered expression of *MIR160a* (*FOC*) and the accumulation of mature miR160 affected the miR160 target genes *ARF10, -16, and -17*, we carried out RT-PCR and quantitative real time RT-PCR experiments. Compared with wild-type expression levels, the RT-PCR results showed that expression of *ARF10, -16, and -17* was increased in most examined *foc* organs, particularly in young seedlings, inflorescences and mature leaves (Figure S5b). In addition, the quantitative real time RT-PCR results demonstrated that *ARF10, -16, and -17* were expressed at significantly higher levels in young *foc* seedlings and inflorescences, relative to their levels in the wild type (Figure S5c). Our results suggest that the impaired function of *MIR160a* results in increased expression of *ARF10, -16, and -17* in *foc* plants.

We further examined expression of *MIR160a* and *ARF10, -16, and -17* during embryonic development in wild-type and
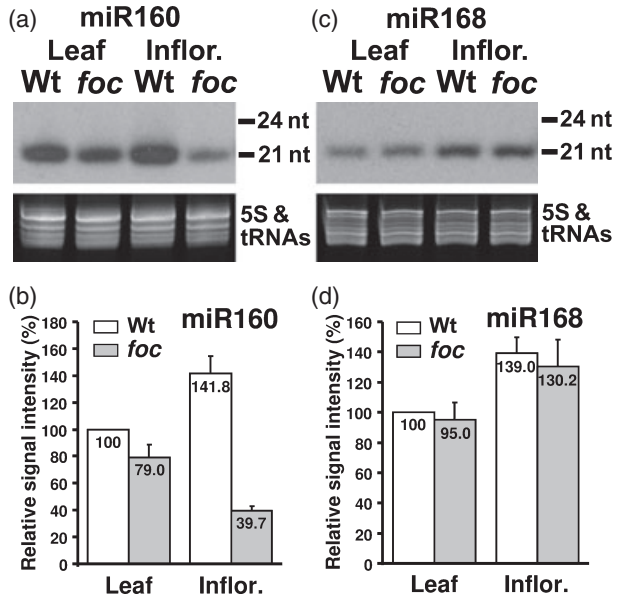
Figure 4. RNA blot assays showed that accumulation of mature miR160 was decreased in *foc* plants.
(a) A representative RNA gel blot image (top) showing that accumulation of mature miR160 was considerably reduced in *foc* leaves and inflorescences. Ethidium bromide staining of 5S rRNA and tRNAs are shown as loading controls (bottom).
(b) A diagram showing that accumulation of miR160 is more significantly reduced in *foc* inflorescences than in *foc* leaves. Signals from wild-type leaves were set as 100%. Bars indicate standard deviation.
(c), (d) The accumulation of miR168 was not significantly changed in *foc* leaves or inflorescences.
Abbreviations: Inflor., inflorescence; wt, wild type.

foc plants using *in situ* hybridization. In the wild type, the expression of *MIR160a* was uniformly detected using the *MIR160a* antisense probe in the embryo proper at the octant and dermatogen stages (Figure 5a,b), while the expression of *MIR160a* was stronger in whole embryos at the globular and triangular stages (Figure 5c,d). At the heart stage, *MIR160a* was primarily expressed in cotyledon primordia and in the vascular primordium (Figure 5e). At the torpedo stage, the *MIR160a* expression was decreased and was mostly in the cotyledons and hypocotyl epidermal cells (Figure 5f). In *foc* embryos, *MIR160a* was almost undetectable (Figure 5g–i).

Expression levels and domains of *ARF16* and *-17* were markedly changed in *foc* plants. Although the expression pattern of *ARF10* remained similar during early stages, after the late heart stage it was expressed at higher levels in *foc* cotyledons than in the wild type (Figure 5k,l). In the wild type, *ARF16* was expressed in the vascular primordium at the globular stage (Figure 5m), in cotyledon primordia and the vascular primordium at the heart stage (Figure 5o), and in cotyledons and the procambium at the late heart stage (Figure 5q). However, in *foc ARF16* expression was greatly increased at the globular stage (Figure 5n), and strongly
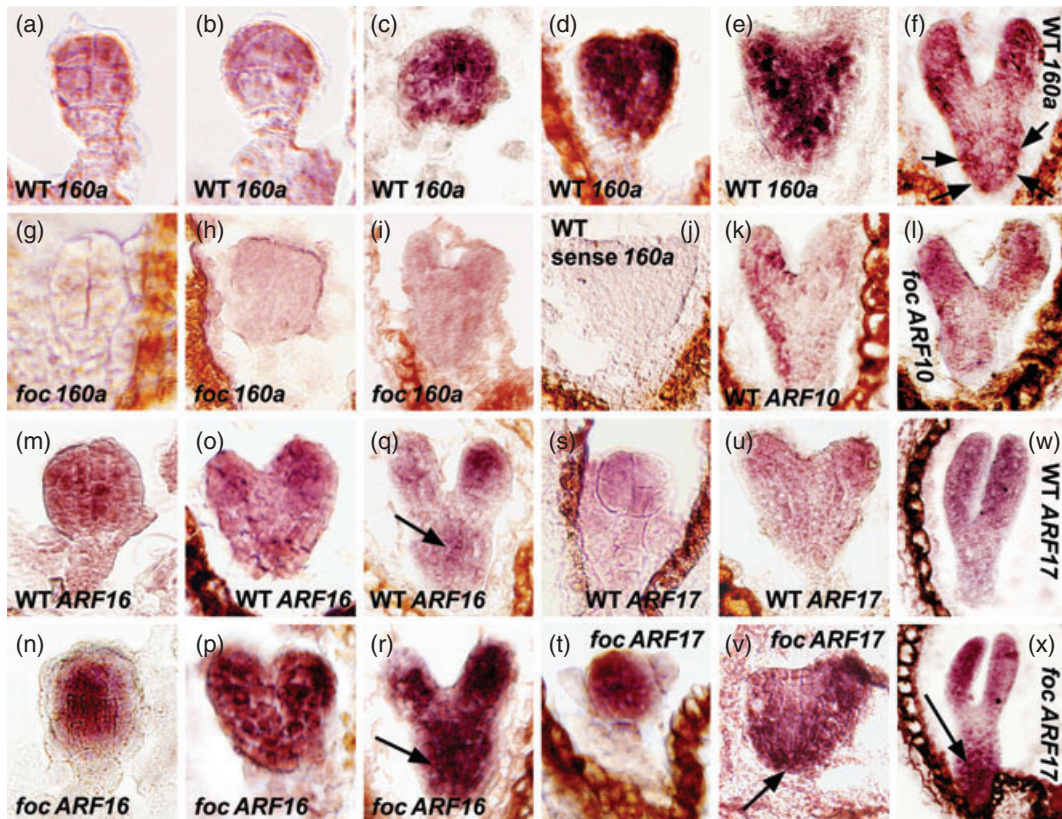
Figure 5. Expression of *ARF10*, *-16*, and *-17* is altered during embryo development in *foc*.
(a, b) Expression of *MIR160a* (*160a* in a–j) was detected in the embryo proper at the octant (a) and dermatogen (b) stages in wild type. (c, d) *MIR160a* was strongly expressed in whole embryos at the globular (c) and triangular (d) stages in the wild type. (e) *MIR160a* expression was primarily expressed in cotyledon primordia and in the vascular primordium at the heart stage in the wild type. (f) *MIR160a* was primarily expressed in cotyledons and epidermal cells in hypocotyl (arrows) at the early torpedo stage in the wild type. (g–i) *MIR160a* was almost undetectable at the octant (g), triangular (h), and late heart (i) stages in *foc*. (j) A wild-type embryo at the heart stage hybridized with the *MIR160a* sense probe, showing no signal. Similar results were observed using sense probes for *ARF10*, *-16*, and *-17* genes (data not shown). (k, l) *ARF10* was expressed at a higher level in *foc* cotyledons (l) relative to the expression in the wild type (k) at the late heart stage. (m, n) The expression of *ARF16* was greatly increased in the vascular primordium in the *foc* embryo (n) relative to expression in the wild type at the globular stage (m). (o, p) *ARF16* was weakly expressed in cotyledon primordia and the vascular primordium at the heart stage in the wild type (o), while *ARF16* was strongly expressed in the whole embryo in *foc* (p). (q, r) *ARF16* expression was greatly increased in cotyledons and procambium (arrows) in *foc* embryos (r) relative to the expression levels in the wild type at the late heart stage (q). (s, t) The *foc* embryo had higher *ARF17* expression (t) than did the wild type at the octant stage (s). (u, v) *ARF17* was mainly detected in cotyledons and the central embryo domain at the heart stage in the wild type (u), while in *foc* *ARF17* was strongly expressed in the basal embryo domain (arrow, v). (w, x) *ARF17* expression became more predominant in *foc* hypocotyls (arrow, x) than in the wild type (w) at the torpedo stage.

expressed in embryos at the heart stage (Figure 5p). In addition, the expression of *ARF16* was substantially increased at the late heart stage, particularly in the procambium (Figure 5r). Relative to expression in the wild type, *ARF17* expression was much stronger at the octant stage in *foc* (Figure 5s,t). *ARF17* was principally expressed in cotyledons and the central embryo domain at the heart stage in the wild type (Figure 5u). However, in *foc* *ARF17* expression was not only increased in cotyledons, but was also strong in the basal embryo domain (Figure 5v). In the wild type, *ARF17* was weakly expressed in the hypocotyl at the torpedo stage (Figure 5w); however, in *foc* it was strongly expressed in the hypocotyl, particularly in the root meristem (Figure 5x). No hybridization was detected when *MIRI60a*, *ARF10*, *-16*, and *-17* sense probes were used (Figure 5; data not shown). Our results indicate that the expression levels and domains of

ARF16 and *-17* are considerably altered in *foc* embryos, which may cause pleiotropic phenotypes in embryo development.

foc is deficient in auxin responses

Auxin is known to play major roles in anther and embryo development (Jenik and Barton, 2005; Cecchetti *et al.*, 2008). The miR160 target genes *ARF10*, *-16*, *-17* are involved in auxin signaling (Mallory *et al.*, 2005; Okushima *et al.*, 2005; Wang *et al.*, 2005; Guilfoyle and Hagen, 2007). Furthermore, expression of *MIR160a* and *ARF10*, *-16*, *-17* was markedly affected in *foc* aerial organs, particularly in reproductive organs. Therefore, we examined the auxin response using *DR5*::GUS as a proxy for auxin levels (Ulmasov *et al.*, 1997). In *DR5*::GUS plants, GUS activity was strong in cotyledons and moderate in the margin and veins of mature leaves (data not
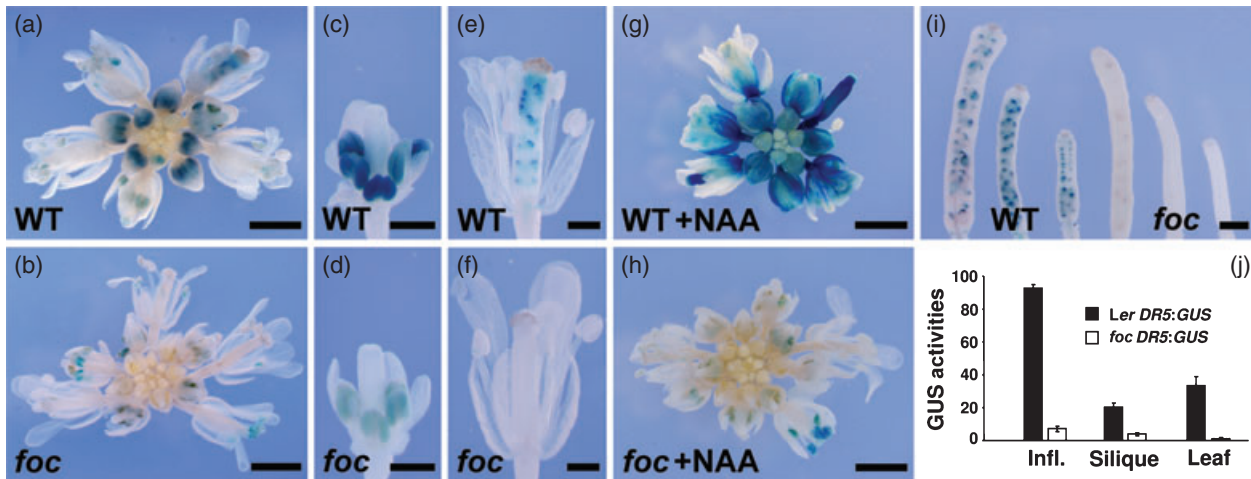
Figure 6. *foc* is defective in the auxin signaling response.
(a, b) Inflorescences showing GUS expression in young buds and open flowers in wild type (a), but little or none in *foc* (b). (c, d) Stage 10 buds showing strong GUS expression in wild-type anthers (c), but much weaker expression in *foc* anthers (d). (e, f) Pollinated flowers showing GUS staining in wild-type carpels (e), but no staining in *foc* carpels (f). (g, h) Inflorescences after treatment with 50 μM NAA, showing enhanced and expanded GUS expression in young and old flowers, particularly in sepals and carpels in wild type (g), but no enhancement in *foc* (h). (i) Carpels showing GUS staining in wild-type embryos (left three), but less or no staining in *foc* embryos (right three). (j) The quantification of GUS activity (nM 4-methylumbelliferone (4-MU)/min/mg).
Abbreviations: wild type (WT), *DR5*:GUS plants; *foc*, *foc DR5*:GUS plants; Inf., inflorescence. Scale bars: 1 mm in (a, b), (g–i); 250 μm in (c–f).

shown). However, in *foc DR5*::GUS plants, GUS expression was greatly reduced in those organs (data not shown).

In *DR5*::GUS plants, GUS was strongly expressed in anthers of young buds and carpels of pollinated flowers (Figure 6a,c,e). However, in *foc DR5*::GUS plants GUS expression was greatly reduced in anthers of young buds, and was not detectable in carpels of old flowers (Figure 6b,d,f). Furthermore, compared with *DR5*::GUS expression in the wild type, GUS staining was greatly reduced in *foc* embryos (Figure 6i,j). After treatment with 50 μM 1-naphthalene acetic acid (NAA), the *DR5*:GUS inflorescences showed greatly enhanced GUS expression, indicated by strong staining in both young buds and old flowers, particularly in sepals and carpels (Figure 6g). In contrast, no enhancement of GUS staining was observed in the *foc* background (Figure 6h). Our results indicate that *foc* is defective in auxin signal responses.

Auxin positively regulates expression of *MIR160a*

Three potential AuxREs were found in the 3′ regulatory region of *MIR160a* by searching the PLANTCARE database (http://bioinformatics.psb.ugent.be/webtools/plantcare/html/; Figure 3a), leading to the hypothesis that expression of *MIR160a* might be regulated by auxin. To test this idea, we examined whether exogenous auxin could alter *MIR160a* expression through its 3′ regulatory region. Taking advantage of our *Pro_FOC*:GUS:*3′_FOC* and *Pro_FOC*:GUS transgenic plants, we first treated young seedlings at 5 days after germination (DAG) with 10 μM indole-3-acetic acid (IAA). In *Pro_FOC*:GUS:*3′_FOC* seedlings, IAA treatments caused a large increase in GUS expression in cotyledons after 2, 6 or 12 h (Figure 7a–d), whereas without IAA treatment, GUS

expression levels were only slightly increased in cotyledons (Figure 7e–h). No significant changes in GUS expression were detected with IAA treatments in *Pro_FOC*:GUS seedlings (Figure 7i–p). We obtained similar results using seedlings with true leaves (Figure S7).

To further test whether IAA treatment increased *MIR160a* expression, we performed quantitative real time RT-PCR using young seedlings. Without IAA treatment, *MIR160a* expression was slightly elevated after 0.5 and 1 h, but greatly increased after 2 h (Figure 8a). However, with IAA treatments, the levels of *MIR160a* expression were significantly increased after 0.5, 1.0, and 2.0 h (Figure 8a). In wild-type seedlings, the expression levels of *ARF10*, *-16*, and *-17* did not change greatly after IAA treatment (Figure 8c–e). However, in *foc* seedlings, the expression of *ARF10* was greatly increased after 1.0 h of IAA treatment (Figure 8c), while the expression of *ARF16* and *-17* was significantly increased after 0.5, 1.0, and 2.0 h of IAA treatments (Figure 8d,e). Thus, the steady expression patterns of *ARF10*, *-16*, and *-17* after IAA treatments of wild-type seedlings might be mainly down-regulated by the increased expression of *MIR160a*. In summary, our results indicate that auxin up-regulates expression of *MIR160a* in seedlings, possibly through the AuxREs in its 3′ regulatory region.

DISCUSSION

Regulation of *ARF10, -16,* and *-17* by *MIR160a* in embryo development

We characterized the function of *MIR160a* in regulating plant development, particularly embryogenesis, by analyzing the novel phenotypes of *foc*, the *MIR160a* loss-of-function
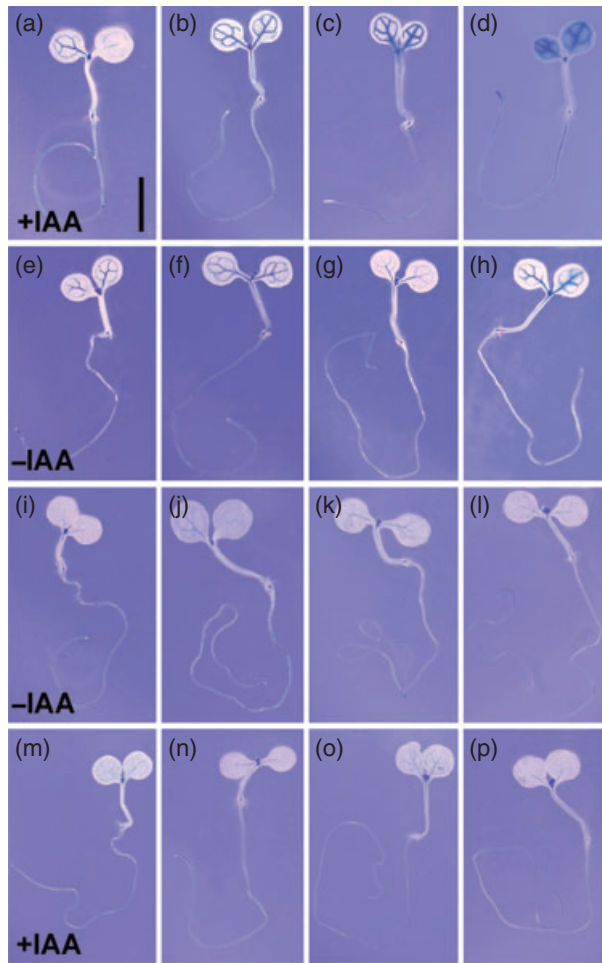
Figure 7. Exogenous auxin regulates expression of *MIR160a* through its 3′ regulatory region.

(a)–(d) *Pro$_{FOC}$*:GUS:*3′$_{FOC}$* seedlings treated with 10 μM of indole-3-acetic acid (IAA) in 1/2 × MS solution for 0 (a), 2 (b), 6 (c), and 12 (d) h showing greatly increased GUS activity in cotyledons.

(e–h) *Pro$_{FOC}$*:GUS:*3′$_{FOC}$* seedlings treated with 1/2 × MS solution for 0 (e), 2 (f), 6 (g), and 12 (h) h showing slightly increased GUS activity over time in cotyledons.

(i–p) *Pro$_{FOC}$*:GUS seedlings treated with 1/2 × MS solution (i–l) or 10 μM IAA (m–p) for 0 (i,m), 2 (j,n), 6 (k,o), and 12 (l,p) h, showing no changes in GUS activity.

Scale bar: 0.5 cm in all panels.

Figure 8. Quantitative real time RT-PCR results show that the expression of *MIR160a* in seedlings is up-regulated by auxin.

Transcripts of seedlings without indole-3-acetic acid (IAA) treatments were used as standards for normalization. *Indicates the difference is significant (*P*-values <0.01 or 0.05). Abbreviations: wt, wild type; h, hour.

(a) The expression of *MIR160a* was significantly increased after 0.5, 1.0, and 2.0 h of IAA treatment.

(b) Expression of *IAA5* was used to confirm that the IAA treatments was effective.

(c–e) Expression of *ARF10*, -*16*, and -*17* remained similar after IAA treatment in wild-type seedlings, while their expression was significantly increased in *foc* seedlings in most of time courses.

mutant in Arabidopsis. Moreover, we demonstrated that the 3′ regulatory region of *MIR160a* is required for its expression pattern and regulation by auxin. The dynamic and differential distribution of auxin activity during embryo development suggests that both ARF activators and repressors are required for embryonic cell patterning in Arabidopsis (Willemsen and Scheres, 2004; Jenik and Barton, 2005; Bowman and Floyd, 2008). Among the available loss-of-function mutants (for at least 18 *ARF* genes), only single mutants of *arf2*, *arf3*, *arf5*, *arf7*, *arf8*, and *arf19* have phenotypes in growth or development, indicating that most *ARF*s

function redundantly (Sessions *et al.*, 1997; Hardtke and Berleth, 1998; Harper *et al.*, 2000; Ellis *et al.*, 2005; Nagpal *et al.*, 2005; Wilmoth *et al.*, 2005; Goetz *et al.*, 2006; Schruff *et al.*, 2006; Okushima *et al.*, 2007). So far, only *ARF5* and -*7* have been found to play direct roles in controlling embryogenesis. *monopteros*/*arf5* is defective in establishing cell division patterns of the embryo proper and of the uppermost cell of the suspensor (Hardtke and Berleth, 1998; Hamann *et al.*, 2002). *ARF5* is expressed in the apical cell and its

daughter cells until the 16-cell stage. *ARF5* expression then becomes restricted to provascular cells. A mutation in *NON-PHOTOTROPIC HYPOCOTYL4* (*ARF7*), the closest homolog of *ARF5*, strongly enhances the *arf5* phenotype (Harper *et al.*, 2000; Hardtke *et al.*, 2004). The extensively overlapping expression patterns of *ARF5* and -*7* further indicate that they function redundantly during embryogenesis. Therefore, ARF5 and -7, serving as potential transcriptional activators, are essential for embryo development.

Our study showed that *ARF10*, -*16*, and -*17*, known to be regulated by *MIR160a*, play important roles in controlling embryogenesis. The *MIR160* gene family consists of three members (*MIR160a*, -*b*, and -*c*). Ectopic expression of *MIR160a*, -*b*, or -*c* causes disorganized root caps and more lateral roots, whereas expression of a miR160 resistant-version of *ARF16* (*mARF16*) results in reduced fertility and fewer lateral roots (Wang *et al.*, 2005). Plants expressing an *mARF17* version exhibited diverse abnormalities in vegetative and reproductive development (Mallory *et al.*, 2005). The aberrant seedlings produced in *mARF17* plants indicate that *ARF17* may control early embryonic development. Analyses using similar approaches revealed that the negative regulation of *ARF10* by miR160 is essential for plant development and ABA signaling (Liu *et al.*, 2007). *foc* plants produce embryos with pleiotropic defects, including abnormal suspensors, no hypophysis, and irregular cell patterning in the central embryo domain. Abnormal cell differentiation in the boundary between the embryo proper and the uppermost suspensor cell may cause some suspensor cells to eventually incorporate into the embryo. It is also possible that *mir160a* embryos are defective in cell patterning in central embryo domains. Our *in situ* hybridization results demonstrate that *MIR160a* is expressed throughout early embryogenesis. Besides greatly increased levels of expression of *ARF16* and -*17*, the expression domain of *ARF17* is shifted in *foc* embryos. Our results show that auxin activity is decreased in *foc*, suggesting that *ARF10*, -*16*, and -*17* may repress auxin signaling. At the triangular and heart stages, auxin activity is mainly detected in cotyledon apices as well as in the hypophysis and its derivatives. Therefore, ARF10, -16, and -17 might contribute as repressors in establishing and maintaining auxin signals in embryogenesis. In summary, our results provide insight into the molecular mechanism of embryo development involving *ARF*s, which are regulated by *MIR160a*.

Regulation of *MIR160a* expression by auxin

Transcriptional and post-transcriptional controls of *MIR* expression have not been extensively studied, although the spatial and temporal actions of miRNAs are critical for their function. The levels of mature miRNAs are determined by their transcription, processing, and incorporation into the RISC. Previous experiments show that the level of miR164 increased after treatment with 10 μM NAA (Guo *et al.*, 2005), while changes in miR160, miR164, or miR167 were not detected after treatment with 10 μM IAA (Mallory *et al.*, 2005). The level of *ARF17* mRNA also remained unchanged (Mallory *et al.*, 2005). In seedlings, exogenous IAA induces a slow increase in *ARF16* expression, followed by a substantial increase after 5 h (Wang *et al.*, 2005). Microarray analyses showed that expression of *ARF10*, -*16*, and -*17* remain at similar levels before and after 1 and 3 h of IAA treatment (Goda *et al.*, 2004, 2008; Paponov *et al.*, 2008). Our quantitative RT-PCR results agree with previous findings when the seedlings were treated with 10 μM IAA. However, the overall expression of *ARF10*, -*16*, and -*17* was substantially increased after treatments with 10 μM IAA in *foc* seedlings, suggesting that the increased expression of *MIR160a* induced by IAA treatment down-regulates expression of *ARF10*, -*16*, and -*17*. We also found that *MIR160a* expression in inflorescences is up-regulated by IAA (data not shown). Three potential AuxREs in the 3′ regulatory region of *MIR160a* might be required for regulating the expression of *MIR160a* by auxin. Taken together, the spatial and temporal expression of *MIR160a* may be sophisticatedly regulated by the 5′ promoter and 3′ regulatory region, as well as by the local concentration of auxin.

Functional analysis of *MIR160* genes using the loss-of-function approach

Our study demonstrated a specific function for *MIR160a* using a loss-of-function approach. *MIR160a* (*At2g39175*), -*b* (*At4g17788*), and -*c* (*At5g46845*) may play different roles in regulating the miR160 target genes *ARF10*, -*16*, and -*17*. In the *MIR164* family, single loss-of-function mutants in *mir164a*, -*b*, and -*c* showed subtle but different phenotypes in flower development or lateral root formation (Baker *et al.*, 2005; Guo *et al.*, 2005). However, the *mir164abc* triple mutant exhibited enhanced and novel phenotypes (Sieber *et al.*, 2007). Although gene numbers vary with species, *MIR160* is deeply conserved in the plant kingdom from moss (*Physcomitrella patens*) to higher plants (Axtell *et al.*, 2007). Our phylogenetic analysis using sequences in the stem–loop regions of *MIR160* from different plant species showed that Arabidopsis *MIR160b* and -*c* were very similar, but distant from *MIR160a* (data not shown). That the loss-of-function mutation of *MIR160a* alone results in severe phenotypes indicates that *MIR160a* may play a primary role in regulating plant development. Resistant versions of *ARF10*, -*16*, and -*17* interfere with the recognition of miR160s derived from all three *MIR160* genes (Mallory *et al.*, 2005; Wang *et al.*, 2005; Liu *et al.*, 2007). In the loss-of-function *foc* mutant, the altered expression of *ARF10*, -*16*, and -*17* was affected only by miR160 derived from *MIR160a*. In addition, expression of *ARF10*, -*16*, and -*17* was affected simultaneously in *foc*, which resulted in severe and novel phenotypes. It will be interesting to study the specific function of *MIR160b* and -*c* using the loss-of-function approach, and to test the

possibilities of specialization and redundancy among the three *MIR160* genes in Arabidopsis.

EXPERIMENTAL PROCEDURES

Plant materials and growth conditions

The *Arabidopsis thaliana foc* mutant is in the Landsberg *erecta* background. *foc* was also backcrossed to the Columbia (Col-0) ecotype. The *DR5::*GUS line was kindly provided by Dr Thomas Guilfoyle (University of Missouri, Columbia, Missouri). Plants were grown on Metro-Mix 360 soil at 22°C under 16 h of light/8 h of dark or 8 h of light/16 h of dark.

Identification of *FOC*

To identify *FOC*, TAIL-PCR was performed using *foc* genomic DNA (Table S1) (Liu *et al.*, 1995; Zhao *et al.*, 2002). The full-length cDNA of *MIRNA160a* was obtained by RACE-PCR. The RACE-PCR products were cloned into the pGEM-T Easy vector (Promega, http://www.promega.com/) and sequenced.

Phenotypic analyses and microscopy

Micrographs were taken with an Olympus DP70 digital camera through stereo (Olympus SZX-RFL) and compound (Olympus BX51) microscopes (http://www.olympus.com/). Embryo development was analyzed using a whole-mount squash method essentially as previously described (Schneitz *et al.*, 1995; Blilou *et al.*, 2005; Zhou *et al.*, 2009). Siliques between 1 and 7 DAP were fixed overnight in FAA [50% (w/v) ethanol, 5% (w/v) acetic acid, and 3.7% (w/v) form-aldehyde] at 4°C. After rehydration in an ethanol series, siliques were transferred onto a slide and ovules were dissected in Hoyer's buffer (70% chloral hydrate and 4% glycerol). Samples for scanning electron microscopy (SEM) were prepared and examined as previously described using a Hitachi S-570 scanning electron microscope (http://www.hitachi.com/) (Bowman *et al.*, 1989; Zhao *et al.*, 2001).

Vector construction and plant transformation

All DNA and cDNA fragments were PCR-amplified by Phusion High-fidelity DNA polymerase (New England Biolabs, http://www.neb.com/) (Table S1), then cloned into the pENTR™ TOPO® vector (Invitrogen, http://www.invitrogen.com/), and finally introduced into Gateway binary vectors using the Gateway® LR recombinase II enzyme mix (Invitrogen). Plant transformation was performed using *Agrobacterium tumefaciens* strain GV3101 (Clough and Bent, 1998). Transformants were screened on 1/2 × MS agar plates containing kanamycin (50 mg/L) and hygromycin (50 mg/L).

For complementation experiments, two constructs were generated by cloning a 4921-bp genomic fragment of *FOC* (*At2g39175*, *ETB*) and a 3820-bp genomic fragment of *At2g39170* (*ETA*). To examine regulation of *FOC* expression, three constructs were generated: *Pro~FOC~*:GUS:*3′~FOC~*, *Pro~FOC~*:GUS:*Δ3′~FOC~*, and *Pro~FOC~*:GUS. Based on the sequence of the *FOC* transcript and the *Ds* location, a 1502-bp fragment was used as the *FOC* promoter, while 2488-bp and 1456-bp fragments were used as the *FOC* 3′ regions for *Pro~FOC~*:GUS:*3′~FOC~* and *Pro~FOC~*:GUS:*Δ3′~FOC~* constructs, respectively. The *FOC* promoter was introduced into the Gateway pGWB3 binary vector with the GUS gene, then the *FOC* 3′ fragments were cloned into a *Sac*I site downstream of the GUS gene.

Hormone Treatments

Five-day-old *Pro~FOC~*:GUS:*3′~FOC~* and *Pro~FOC~*:GUS T$_2$ transgenic seedlings were transferred onto Whatman filter paper soaked with 1/2 × MS liquid media containing 10 μM IAA and 0.1% ethanol in a Petri dish. Mock treatments were performed using the same solution but without IAA. Seedlings were collected at 0, 2, 6, and 12 h for GUS staining. For quantitative real time RT-PCR, 5-day-old wild-type and *foc* seedlings were treated similarly, and then collected at 0, 0.5, 1, and 2 h for total RNA extraction. For NAA treatment, *DR5*:GUS and *foc DR5*:GUS inflorescences were incubated with 50 μM NAA in 0.01% Silwet L-77 and 0.1% ethanol in the morning, and collected for GUS staining after 6 h. Mock treatments were performed with the same solution lacking NAA.

GUS staining and GUS activity assay

Histochemical GUS staining (Willemsen *et al.*, 1998) and GUS activity assays (Jefferson *et al.*, 1987) were performed essentially as described previously. For the GUS activity assay, fluorescence was determined using a Synergy HT multi-mode microplate reader at 360 nm (excitation) and 460 nm (emission) (BioTek, http://www.biotek.com). Protein concentration was measured using the Bradford method and GUS activity was calculated as nmol 4-methylumbelliferone (4-MU)/min/mg protein.

Small RNA northern blots

Small RNA Northern blot assays were carried out essentially as described (Xie, 2010). Briefly, total RNA extracts (15 μg) were resolved in a 17% polyacrylamide gel containing 7 M urea, transferred to Nytran SuPerCharge nylon membrane (Whatman, http://www.whatman.com/), and then probed with ^{32}P-labeled oligonucleotides with a sequence complementary to the target small RNAs. To enhance detection sensitivity, locked nucleic acid (LNA)-modified (Valoczi *et al.*, 2004) oligonucleotides (Exiqon, http://www.exiqon.com/) specific for miR160 (a gift from James Carrington, Oregon State University, Corvallis, OR, USA), miR168, and miR171, respectively, were used as probes. Two RNA oligos of 21 and 24 nucleotides were used as size markers. Before exposure of the blots to X-ray films, radioactive signals from blots were captured in a phosphorimager (Storm, Amersham Biosciences, http://www1.gelifesciences.com) and analyzed using ImageQuant software.

RNA *in situ* hybridization

RNA *in situ* hybridizations were performed on wild-type and *foc* silique sections essentially as described (Long and Barton, 1998; Zhao *et al.*, 2002). The 5′ region upstream stem loop of *MIR160a*, as well as specific cDNAs of *ARF10*, -*16* and -*17* were PCR-amplified (Table S1) and then cloned into the pGEM®-T Easy Vector (Promega). Antisense and sense probes were synthesized using the SP6/T7 DIG RNA Labeling Kit (Roche, http://www.roche.com/).

RT-PCR and quantitative real time RT-PCR

Total RNAs were extracted from different plant tissues using the RNeasy Plant Mini Kit (Qiagen, http://www.qiagen.com/). The RNA concentrations were measured with a NanoDrop ND-1000 spectrophotometer (Thermo Scientific, http://www.nanodrop.com). Reverse transcription reactions were carried out using a QuantiTect Reverse Transcription Kit (Qiagen). The PCR and quantitative real time PCR (DNA Engine Opticon 2 system) were performed using primers as noted for specific experiments (Table S1). *ACTIN2* was used as an internal control. Fast SYBR Green PCR Master Mix (Applied Biosystems, http://www3.appliedbiosystems.com/) was used for quantitative real-time PCRs. The quantitative RT-PCR results were analyzed as described previously (Pfaffl *et al.*, 2002). Three independent experiments were carried out. Each value indicates the average and a standard error.

ACKNOWLEDGEMENTS

SUPPORTING INFORMATION

Additional Supporting Information may be found in the online version of this article:

Figure S1. *foc* has defective leaf development.
Figure S2. *foc* has defective flower development.
Figure S3. *foc* has abnormal seed development.
Figure S4. *foc* seedlings showing diverse defects in development.
Figure S5. Cloning of *FOC* and expression of *FOC* and miR160 target genes.
Figure S6. Sequence of full-length *MIR160a* cDNA.
Figure S7. Exogenous auxin increases expression of *MIR160a*.
Table S1. A list of primers used in this study.

Please note: As a service to our authors and readers, this journal provides supporting information supplied by the authors. Such materials are peer-reviewed and may be re-organized for online delivery, but are not copy-edited or typeset. Technical support issues arising from supporting information (other than missing files) should be addressed to the authors.

REFERENCES

Allen, E., Xie, Z., Gustafson, A.M. and Carrington, J.C. (2005) microRNA-directed phasing during trans-acting siRNA biogenesis in plants. *Cell*, **121**, 207–221.

Allen, R.S., Li, J., Stahle, M.I., Dubroue, A., Gubler, F. and Millar, A.A. (2007) Genetic analysis reveals functional redundancy and the major target genes of the *Arabidopsis* miR159 family. *Proc. Natl Acad. Sci. USA*, **104**, 16371–16376.

Axtell, M.J., Snyder, J.A. and Bartel, D.P. (2007) Common functions for diverse small RNAs of land plants. *Plant Cell*, **19**, 1750–1769.

Baker, C.C., Sieber, P., Wellmer, F. and Meyerowitz, E.M. (2005) The *early extra petals1* mutant uncovers a role for microRNA miR164c in regulating petal number in *Arabidopsis*. *Curr. Biol.* **15**, 303–315.

Bartel, D.P. (2009) MicroRNAs: target recognition and regulatory functions. *Cell*, **136**, 215–233.

Bartel, B. and Bartel, D.P. (2003) MicroRNAs: at the root of plant development? *Plant Physiol.* **132**, 709–717.

Baumberger, N. and Baulcombe, D. C. (2005) *Arabidopsis* ARGONAUTE1 is an RNA Slicer that selectively recruits microRNAs and short interfering RNAs. *Proc. Natl Acad. Sci. USA*, **102**, 11928–11933.

Blilou, I., Xu, J., Wildwater, M., Willemsen, V., Paponov, I., Friml, J., Heidstra, R., Aida, M., Palme, K. and Scheres, B. (2005) The PIN auxin efflux facilitator network controls growth and patterning in *Arabidopsis* roots. *Nature*, **433**, 39–44.

Boutet, S., Vazquez, F., Liu, J., Beclin, C., Fagard, M., Gratias, A., Morel, J.B., Crete, P., Chen, X. and Vaucheret, H. (2003) *Arabidopsis* HEN1: a genetic link between endogenous miRNA controlling development and siRNA controlling transgene silencing and virus resistance. *Curr. Biol.* **13**, 843–848.

Bowman, J.L. and Floyd, S.K. (2008) Patterning and polarity in seed plant shoots. *Annu. Rev. Plant Biol.* **59**, 67–88.

Bowman, J.L., Smyth, D.R. and Meyerowitz, E.M. (1989) Genes directing flower development in *Arabidopsis*. *Plant Cell*, **1**, 37–52.

Carrington, J.C. and Ambros, V. (2003) Role of microRNAs in plant and animal development. *Science*, **301**, 336–338.

Cartolano, M., Castillo, R., Efremova, N., Kuckenberg, M., Zethof, J., Gerats, T., Schwarz-Sommer, Z. and Vandenbussche, M. (2007) A conserved microRNA module exerts homeotic control over *Petunia hybrida* and *Antirrhinum majus* floral organ identity. *Nat. Genet.* **39**, 901–905.

Cecchetti, V., Altamura, M.M., Falasca, G., Costantino, P. and Cardarelli, M. (2008) Auxin regulates *Arabidopsis* anther dehiscence, pollen maturation, and filament elongation. *Plant Cell*, **20**, 1760–1774.

Chen, X. (2008) MicroRNA metabolism in plants. *Curr. Top. Microbiol. Immunol.* **320**, 117–136.

Chitwood, D.H., Nogueira, F.T., Howell, M.D., Montgomery, T.A., Carrington, J.C. and Timmermans, M.C. (2009) Pattern formation via small RNA mobility. *Genes Dev.* **23**, 549–554.

Clough, S.J. and Bent, A.F. (1998) Floral dip: a simplified method for Agrobacterium-mediated transformation of Arabidopsis *thaliana*. *Plant J.* **16**, 735–743.

Ellis, C.M., Nagpal, P., Young, J.C., Hagen, G., Guilfoyle, T.J. and Reed, J.W. (2005) *AUXIN RESPONSE FACTOR1* and *AUXIN RESPONSE FACTOR2* regulate senescence and floral organ abscission in *Arabidopsis thaliana*. *Development*, **132**, 4563–4574.

Fahlgren, N., Montgomery, T.A., Howell, M.D., Allen, E., Dvorak, S.K., Alexander, A.L. and Carrington, J.C. (2006) Regulation of *AUXIN RESPONSE FACTOR3* by TAS3 ta-siRNA affects developmental timing and patterning in *Arabidopsis*. *Curr. Biol.* **16**, 939–944.

Gasciolli, V., Mallory, A.C., Bartel, D.P. and Vaucheret, H. (2005) Partially redundant functions of *Arabidopsis* DICER-like enzymes and a role for DCL4 in producing trans-acting siRNAs. *Curr. Biol.* **16**, 1494–1500.

Goda, H., Sawa, S., Asami, T., Fujioka, S., Shimada, Y. and Yoshida, S. (2004) Comprehensive comparison of auxin-regulated and brassinosteroid-regulated genes in *Arabidopsis*. *Plant Physiol.* **134**, 1555–1573.

Goda, H., Sasaki, E., Akiyama, K. *et al.* (2008) The AtGenExpress hormone and chemical treatment data set: experimental design, data evaluation, model data analysis and data access. *Plant J.* **55**, 526–542.

Goetz, M., Vivian-Smith, A., Johnson, S.D. and Koltunow, A.M. (2006) *AUXIN RESPONSE FACTOR8* is a negative regulator of fruit initiation in Arabidopsis. *Plant Cell*, **18**, 1873–1886.

Grigg, S.P., Canales, C., Hay, A. and Tsiantis, M. (2005) *SERRATE* coordinates shoot meristem function and leaf axial patterning in *Arabidopsis*. *Nature*, **437**, 1022–1026.

Guilfoyle, T.J. and Hagen, G. (2007) Auxin response factors. *Curr. Opin. Plant Biol.* **10**, 453–460.

Guo, H.S., Xie, Q., Fei, J.F. and Chua, N.H. (2005) MicroRNA directs mRNA cleavage of the transcription factor *NAC1* to downregulate auxin signals for Arabidopsis lateral root development. *Plant Cell*, **17**, 1376–1386.

Hamann, T., Benkova, E., Baurle, I., Kientz, M. and Jurgens, G. (2002) The *Arabidopsis BODENLOS* gene encodes an auxin response protein inhibiting *MONOPTEROS*-mediated embryo patterning. *Genes Dev.* **16**, 1610–1615.

Hardtke, C.S. and Berleth, T. (1998) The *Arabidopsis* gene *MONOPTEROS* encodes a transcription factor mediating embryo axis formation and vascular development. *EMBO J.* **17**, 1405–1411.

Hardtke, C.S., Ckurshumova, W., Vidaurre, D.P., Singh, S.A., Stamatiou, G., Tiwari, S.B., Hagen, G., Guilfoyle, T.J. and Berleth, T. (2004) Overlapping and non-redundant functions of the Arabidopsis auxin response factors MONOPTEROS and NONPHOTOTROPIC HYPOCOTYL 4. *Development*, **131**, 1089–1100.

Harper, R.M., Stowe-Evans, E.L., Luesse, D.R., Muto, H., Tatematsu, K., Watahiki, M.K., Yamamoto, K. and Liscum, E. (2000) The *NPH4* locus encodes the auxin response factor ARF7, a conditional regulator of differential growth in aerial Arabidopsis tissue. *Plant Cell*, **12**, 757–770.

Jefferson, R.A., Kavanagh, T.A. and Bevan, M.W. (1987) GUS fusions: beta-glucuronidase as a sensitive and versatile gene fusion marker in higher plants. *EMBO J.* **6**, 3901–3907.

Jenik, P.D. and Barton, M.K. (2005) Surge and destroy: the role of auxin in plant embryogenesis. *Development*, **132**, 3577–3585.

Jia, G., Liu, X., Owen, H.A. and Zhao, D. (2008) Signaling of cell fate determination by the TPD1 small protein and EMS1 receptor kinase. *Proc. Natl Acad. Sci. USA*, **105**, 2220–2225.

Jones-Rhoades, M. W., Bartel, D.P. and Bartel, B. (2006) MicroRNAs and their regulatory roles in plants. *Annu. Rev. Plant Biol.* **57**, 19–53.

Kidner, C.A. and Martienssen, R.A. (2004) Spatially restricted microRNA directs leaf polarity through ARGONAUT. *Nature*, **428**, 81–84.

Kurihara, Y. and Watanabe, Y. (2004) *Arabidopsis* micro-RNA biogenesis through Dicer-like 1 protein functions. *Proc. Natl Acad. Sci. USA*, **101**, 12753–12758.

Laux, T., Wurschum, T. and Breuninger, H. (2004) Genetic regulation of embryonic pattern formation. *Plant Cell*, **16**(Suppl), S190–S202.

Liu, Y.G., Mitsukawa, N., Oosumi, T. and Whittier, R.F. (1995) Efficient isolation and mapping of Arabidopsis *thaliana* T-DNA insert junctions by thermal asymmetric interlaced PCR. *Plant J.* **8**, 457–463.

Liu, P.P., Montgomery, T.A., Fahlgren, N., Kasschau, K.D., Nonogaki, H. and Carrington, J.C. (2007) Repression of *AUXIN RESPONSE FACTOR10* by microRNA160 is critical for seed germination and post-germination stages. *Plant J.* **52**, 133–146.

Long, J.A. and Barton, M.K. (1998) The development of apical embryonic pattern in *Arabidopsis*. *Development*, **125**, 3027–3035.

Mallory, A.C., Bartel, D.P. and Bartel, B. (2005) MicroRNA-directed regulation of Arabidopsis *AUXIN RESPONSE FACTOR17* is essential for proper development and modulates expression of early auxin response genes. *Plant Cell*, **17**, 1360–1375.

Miska, E.A., Alvarez-Saavedra, E., Abbott, A.L., Lau, N.C., Hellman, A.B., McGonagle, S.M., Bartel, D.P., Ambros, V.R. and Horvitz, H.R. (2007) Most *Caenorhabditis elegans* microRNAs are individually not essential for development or viability. *PLoS Genet.* **3**, 2395–2403.

Mockaitis, K. and Estelle, M. (2008) Auxin receptors and plant development: a new signaling paradigm. *Annu. Rev. Cell Dev. Biol.* **24**, 55–80.

Nag, A., King, S. and Jack, T. (2009) miR319a targeting of *TCP4* is critical for petal growth and development in *Arabidopsis*. *Proc. Natl Acad. Sci. USA*, **106**, 22534–22539.

Nagpal, P., Ellis, C.M., Weber, H. et al. (2005) Auxin response factors *ARF6* and *ARF8* promote jasmonic acid production and flower maturation. *Development*, **132**, 4107–4118.

Okushima, Y., Overvoorde, P.J., Arima, K. et al. (2005) Functional genomic analysis of the *AUXIN RESPONSE FACTOR* gene family members in Arabidopsis *thaliana*: unique and overlapping functions of *ARF7* and *ARF19*. *Plant Cell*, **17**, 444–463.

Okushima, Y., Fukaki, H., Onoda, M., Theologis, A. and Tasaka, M. (2007) ARF7 and ARF19 regulate lateral root formation via direct activation of *LBD/ASL* genes in Arabidopsis. *Plant Cell*, **19**, 118–130.

Paponov, I.A., Paponov, M., Teale, W., Menges, M., Chakrabortee, S., Murray, J.A. H. and Palme, K. (2008) Comprehensive transcriptome analysis of auxin responses in *Arabidopsis*. *Mol. Plant*, **1**, 321–337.

Park, W., Li, J., Song, R., Messing, J. and Chen, X. (2002) CARPEL FACTORY, a Dicer homolog, and HEN1, a novel protein, act in microRNA metabolism in *Arabidopsis thaliana*. *Curr. Biol.* **12**, 1484–1495.

Pfaffl, M.W., Horgan, G.W. and Dempfle, L. (2002) Relative expression software tool (REST) for group-wise comparison and statistical analysis of relative expression results in real-time PCR. *Nucleic Acids Res.* **30**, e36.

Schneitz, K. H., Hülskamp, M. and Pruitt, R.E. (1995) Wild-type ovule development in *Arabidopsis thaliana* – a light microscope study of cleared whole-mount tissue. *Plant J.* **7**, 731–749.

Schruff, M.C., Spielman, M., Tiwari, S., Adams, S., Fenby, N. and Scott, R.J. (2006) The *AUXIN RESPONSE FACTOR 2* gene of *Arabidopsis* links auxin signalling, cell division, and the size of seeds and other organs. *Development*, **133**, 251–261.

Sessions, A., Nemhauser, J.L., McColl, A., Roe, J. L., Feldmann, K.A. and Zambryski, P.C. (1997) ETTIN patterns the *Arabidopsis* floral meristem and reproductive organs. *Development*, **124**, 4481–4491.

Sieber, P., Wellmer, F., Gheyselinck, J., Riechmann, J.L. and Meyerowitz, E.M. (2007) Redundancy and specialization among plant microRNAs: role of the MIR164 family in developmental robustness. *Development*, **134**, 1051–1060.

Song, L., Han, M.H., Lesicka, J. and Fedoroff, N. (2007) *Arabidopsis* primary microRNA processing proteins HYL1 and DCL1 define a nuclear body distinct from the Cajal body. *Proc. Natl Acad. Sci. USA*, **104**, 5437–5442.

Sundaresan, V., Springer, P., Volpe, T., Haward, S., Jones, J.D., Dean, C., Ma, H. and Martienssen, R. (1995) Patterns of gene action in plant development revealed by enhancer trap and gene trap transposable elements. *Genes Dev.* **9**, 1797–1810.

Tiwari, S.B., Hagen, G. and Guilfoyle, T. (2003) The roles of auxin response factor domains in auxin-responsive transcription. *Plant Cell*, **15**, 533–543.

Ulmasov, T., Murfett, J., Hagen, G. and Guilfoyle, T.J. (1997) Aux/IAA proteins repress expression of reporter genes containing natural and highly active synthetic auxin response elements. *Plant Cell*, **9**, 1963–1971.

Ulmasov, T., Hagen, G. and Guilfoyle, T.J. (1999) Activation and repression of transcription by auxin-response factors. *Proc. Natl Acad. Sci. USA*, **96**, 5844–5849.

Valoczi, A., Hornyik, C., Varga, N., Burgyan, J., Kauppinen, S. and Havelda, Z. (2004) Sensitive and specific detection of microRNAs by Northern blot analysis using LNA-modified oligonucleotide probes. *Nucleic Acids Res.* **32**, e175.

Vaucheret, H., Vazquez, F., Crete, P. and Bartel, D.P. (2004) The action of ARGONAUTE1 in the miRNA pathway and its regulation by the miRNA pathway are crucial for plant development. *Genes Dev.* **18**, 1187–1197.

Voinnet, O. (2009) Origin, biogenesis, and activity of plant microRNAs. *Cell*, **136**, 669–687.

Wang, J.W., Wang, L.J., Mao, Y.B., Cai, W.J., Xue, H.W. and Chen, X.Y. (2005) Control of root cap formation by MicroRNA-targeted auxin response factors in Arabidopsis. *Plant Cell*, **17**, 2204–2216.

West, M. and Harada, J.J. (1993) Embryogenesis in higher plants: an overview. *Plant Cell*, **5**, 1361–1369.

Willemsen, V. and Scheres, B. (2004) Mechanisms of pattern formation in plant embryogenesis. *Annu. Rev. Genet.* **38**, 587–614.

Willemsen, V., Wolkenfelt, H., de Vrieze, G., Weisbeek, P. and Scheres, B. (1998) The *HOBBIT* gene is required for formation of the root meristem in the *Arabidopsis* embryo. *Development*, **125**, 521–531.

Williams, L., Carles, C.C., Osmont, K.S. and Fletcher, J.C. (2005) A database analysis method identifies an endogenous trans-acting short-interfering RNA that targets the *Arabidopsis ARF2, ARF3,* and *ARF4* genes. *Proc. Natl Acad. Sci. USA*, **102**, 9703–9708.

Wilmoth, J.C., Wang, S., Tiwari, S.B., Joshi, A.D., Hagen, G., Guilfoyle, T.J., Alonso, J.M., Ecker, J.R. and Reed, J.W. (2005) NPH4/ARF7 and ARF19 promote leaf expansion and auxin-induced lateral root formation. *Plant J.* **43**, 118–130.

Wu, M.F., Tian, Q. and Reed, J.W. (2006) *Arabidopsis* microRNA167 controls patterns of *ARF6* and *ARF8* expression, and regulates both female and male reproduction. *Development*, **133**, 4211–4218.

Wu, G., Park, M.Y., Conway, S.R., Wang, J.W., Weigel, D. and Poethig, R.S. (2009) The sequential action of miR156 and miR172 regulates developmental timing in *Arabidopsis*. *Cell*, **138**, 750–759.

Xie, Z. (2010) Piecing the puzzle together: genetic requirements for miRNA biogenesis in *Arabidopsis thaliana*. In *Plant microRNAs: Methods and Protocols* (Meyers, B.C. and Green, P.J., eds). *Methods Mol. Biol.* **592**, 1–17.

Yang, L., Liu, Z., Lu, F., Dong, A. and Huang, H. (2006) SERRATE is a novel nuclear regulator in primary microRNA processing in Arabidopsis. *Plant J.* **47**, 841–850.

Yu, B., Bi, L., Zheng, B. et al. (2008) The FHA domain proteins DAWDLE in *Arabidopsis* and SNIP1 in humans act in small RNA biogenesis. *Proc. Natl Acad. Sci. USA*, **105**, 10073–10078.

Zhao, D., Yu, Q., Chen, M. and Ma, H. (2001) The *ASK1* gene regulates B function gene expression in cooperation with *UFO* and *LEAFY* in *Arabidopsis*. *Development*, **128**, 2735–2746.

Zhao, D.Z., Wang, G.F., Speal, B. and Ma, H. (2002) The *EXCESS MICROSPOROCYTES1* gene encodes a putative leucine-rich repeat receptor protein kinase that controls somatic and reproductive cell fates in the *Arabidopsis* anther. *Genes Dev.* **16**, 2021–2031.

Zhou, Y., Zhang, X., Kang, X., Zhao, X. and Ni, M. (2009) SHORT HYPOCOTYL UNDER BLUE1 associates with *MINISEED3* and *HAIKU2* promoters *in vivo* to regulate Arabidopsis seed development. *Plant Cell*, **21**, 106–117.